

Communication-Efficient, 2D Parallel Stochastic Gradient Descent for Distributed-Memory Optimization

Aditya Devarakonda
devaraa@wfu.edu
Wake Forest University

Ramakrishnan Kannan
kannanr@ornl.gov
Oak Ridge National Laboratory

Abstract

Distributed-memory implementations of numerical optimization algorithm, such as stochastic gradient descent (SGD), require interprocessor communication at every iteration of the algorithm. On modern distributed-memory clusters where communication is more expensive than computation, the scalability and performance of these algorithms are limited by communication cost. This work generalizes prior work on 1D s -step SGD and 1D Federated SGD with Averaging (FedAvg) to yield a 2D parallel SGD method (HybridSGD) which attains a continuous performance trade off between the two baseline algorithms. We present theoretical analysis which show the convergence, computation, communication, and memory trade offs between s -step SGD, FedAvg, 2D parallel SGD, and other parallel SGD variants. We implement all algorithms in C++ and MPI and evaluate their performance on a Cray EX supercomputing system. Our empirical results show that HybridSGD achieves better convergence than FedAvg at similar processor scales while attaining speedups of $5.3\times$ over s -step SGD and speedups up to $121\times$ over FedAvg when used to solve binary classification tasks using the convex, logistic regression model on datasets obtained from the LIBSVM repository.

1 Introduction

Numerical optimization algorithms are critical to solving large-scale scientific and machine learning problems. As the volume of data continues to rapidly increase, the development of scalable parallel optimization algorithms is critical to solving large-scale optimization problems. In this work, we focus primarily on designing efficient stochastic gradient descent (SGD) algorithms for solving distributed-memory binary classification tasks using the logistic regression model.

One of the primary bottlenecks to scaling SGD on distributed-memory machines is the cost of interprocessor communication at every iteration. Significant prior results have been developed with the goal of reducing communication cost through various algorithmic reorganization techniques (which we describe in Section 2). In this work, we propose to generalize prior efforts in order to develop a more scalable variant of SGD by leveraging a 2D processor grid. This 2D processor grid approach allows us to integrate the best features of existing communication-efficient SGD variants in order to utilize modern multi-threaded, multi-core hardware more efficiently.

We are specifically interested in combining prior work on communication-avoiding algorithms, which aim to reduce communication cost without sacrificing convergence behavior, with prior work on communication efficient algorithms, which aim to reduce communication cost by relaxing convergence behavior/accuracy requirements. Both approaches yield efficient SGD methods with unique convergence, computation, and communication tradeoffs through the use of 1D processor layouts to achieve scalability across multiple processors. Our work exploits the fact that communication-avoiding and communication-efficient approaches distribute the input matrix using distinct partitioning scheme (e.g. partitioning row-wise vs.

column-wise). We exploit these differences in partitioning schemes to develop a generalized, 2D parallel SGD method which combines the two algorithm design methodologies to yield better performance and scalability on modern distributed-memory parallel hardware.

The contributions of this work are:

1. The design of HybridSGD, a 2D parallel SGD method which generalizes existing work on s -step SGD [12] and FedAvg [27] by leveraging a 2D processor grid.
2. Theoretical parallel cost analysis (using Hockney’s communication cost model) which proves bounds on convergence computation, bandwidth, and latency to highlight the theoretical tradeoffs of the proposed HybridSGD method in comparison to parallel SGD, s -step SGD, and FedAvg.
3. Practical distributed-memory parallel implementations of all algorithms in C++ using MPI for parallel processing and Intel OneAPI for dense and sparse BLAS routines.
4. Empirical convergence and performance evaluation of HybridSGD in comparison to existing state-of-the-art distributed-memory implementations which show that HybridSGD achieves speedups of up to $5.3\times$ over communication-avoiding, s -step SGD and speedups up to $121\times$ over communication-efficient FedAvg on a Cray EX supercomputing system.

2 Background

We briefly survey existing approaches to parallelizing and scaling iterative optimization algorithms. These algorithms can broadly be characterized along two dimensions: (1) parallel algorithms which maintain the convergence behavior of sequential variants up to floating-point error (Section 2.1) and (2) parallel algorithms that trade convergence/accuracy for better performance (Section 2.2).

2.1 s -step methods

s -step methods were developed to address the frequency of inter-process synchronization in iterative methods for numerical linear algebra. This initial effort [6, 18, 9, 7, 8] focused on deriving s -step variants of Krylov methods for solving systems of linear equations and singular value problems. This work showed that the vector recurrences in Krylov methods can be unrolled by s iterations, where s is a tunable hyperparameter, and the remaining computations rearranged in order to decrease the frequency of interprocess communication at the expense of additional computation. Subsequent work by Hoemmen [16] developed additional computational kernels (e.g. matrix-powers kernel and tall-skinny QR factorization) to further reduce communication when constructing the Krylov basis and during orthogonalization of the Krylov basis vectors. Despite these algorithmic and practical improvements, the numerical stability of s -step Krylov methods was not established until Carson [1, 2, 3, 4] proved error bounds and developed error correction strategies in order to stabilize s -step Krylov methods. Additional work [29] develop parallel implementations of s -step Krylov methods (specifically, s -step BiCGSTAB) as a solver for algebraic multigrid problems. This application of s -step BiCGSTAB showed practical speedups of up to $2.5\times$ on a real multigrid application.

The s -step technique was more recently generalized to nonlinear, convex optimization problems [24, 26, 13, 14, 13, 12, 11, 32] with a focus on improving the communication efficient of stochastic optimization methods such as randomized coordinate descent (CD) [32, 11, 13, 14, 24], stochastic gradient descent (SGD) [12], and subsampled Newton’s method (SN) [26]. These generalizations of the s -step technique empirically showed that the newly designed variants are numerical stable and could yield speedups up to $5\times$ over existing non s -step solvers in parallel cluster and cloud environments. Note that the primary algorithm

design focus of this line of s -step methods work focused on improving parallel performance without altering convergence behavior or solution accuracy. In some cases, such as for s -step Krylov methods, additional stabilizing techniques were required to ensure numerical stability.

2.2 Communication-efficient methods

Alternative approaches to reducing inter-process communication have also been developed. These techniques typically relax requirements on sequential consistency and/or solution accuracy in order to achieve high performance in shared-memory, distributed-memory, and cloud settings. For example, the work on asynchronous optimization methods [31, 21, 23] derive shared-memory, parallel randomized CD and SGD methods which eliminate blocking inter-process synchronizations. Blocking communication is necessary when solution vector updates are performed in order to avoid race conditions (e.g. where stale values are utilized in the next iteration). However, by introducing asynchronous solution updates, parallel performance can be significantly improved at the expense of sequential consistency and solution accuracy. This prior work showed that when the solution updates are sparse (i.e. threads update disjoint entries), then convergence can be guaranteed.

In the distributed-memory setting, approximate methods such as low-rank decomposition [10] and local optimization [25, 19, 27, 30] has been leveraged to reduce inter-process communication. Work by Chavez and others [10] exploited hierarchical low-rank structure in kernel matrices arising in kernel ridge regression (KRR) problems in order to reduce computation and communication costs at the expense of introducing an approximation error through the use of a rank hyperparameter. Note that if the rank is set to the dimension of the kernel matrix, then a parallel implementation of the classical KRR algorithm can be recovered. A similar approach has been develop in the context of solving kernel SVM problems [30] where a parallel K-means clustering step is used to redistribute the input data such that samples are assigned to processors according to cluster membership. Theoretically, this approach eliminates communication when each processor is assigned disjoint subsets of clusters. In practice, cluster overlap may occur due to load imbalance, therefore a performance-accuracy tradeoff is introduced.

Local optimization [25, 19, 27, 30] is another approach where training samples are partitioned across processes and where the optimization problem is solved simultaneously on locally stored samples without interprocess communication. This divide and conquer approach forms a global model by averaging or summing local solutions. The frequency of aggregation (i.e. communication) is a hyperparameter which controls convergence delay and performance. Much of federated learning [27] utilizes this divide and conquer approach in order to train machine learning models in a communication-efficient manner. In this work we generalize existing approaches by illustrating that the s -step and communication-efficient approaches can be integrated to yield 2D parallel algorithms which strike a balance between the two approaches in order to achieve greater speedups.

While many alternatives to SGD exist for solving the logistic regression (binary classification) problem, such as for example coordinate descent, iterative re-weighted least-squares, quasi-Newton, and higher-order methods, these methods are not amenable to s -step derivation. This is due to the iterative reweighting of the sparse matrix that is performed at each iteration. Therefore, we focus primarily on SGD in this work. We leave a broader survey of optimization methods for logistic regression and a comparison of scalability for future work.

2.3 Notation

This paper focuses on developing 2D parallel SGD algorithms for large-scale binary classification (i.e. logistic regression). We focus primarily on datasets which can be represented as a sparse matrix and vector pair, (\mathbf{A}, \mathbf{y}) , where $\mathbf{A} \in \mathbb{R}^{m \times n}$ with m samples and n features and the binary labels vector $\mathbf{y} \in \{+1, -1\}^m$.

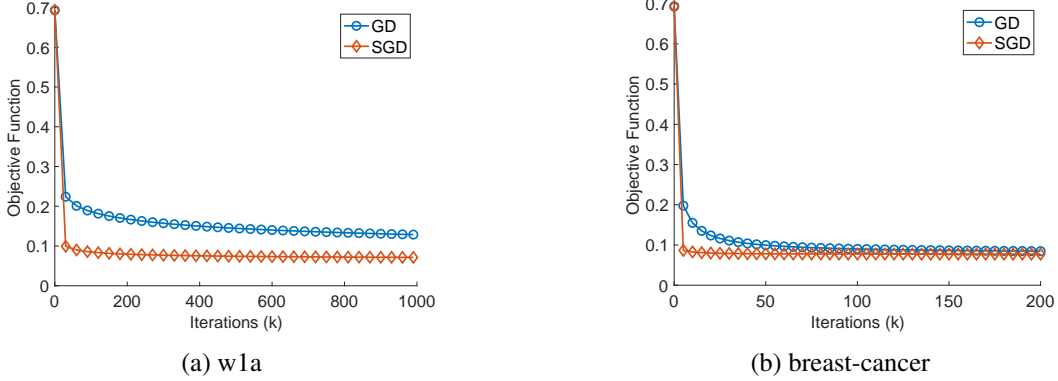


Figure 1: Comparison of convergence behavior of Gradient Descent (GD) and Stochastic Gradient Descent (SGD) for fixed batch size ($b = 16$) and learning rate ($\eta = 1$) on the w1a and breast-cancer datasets. The x-axis was normalized such that every iteration of GD corresponds to m/b iterations of SGD.

We use bold uppercase letters to represent matrices, bold lowercase letters to represent vectors, and nonbold lowercase letters to represent scalar quantities. In addition, all Greek letters represent tunable, scalar quantities. Given that we focus on iterative algorithms in this paper, we use subscripts in two ways: to define a matrix or vector quantity at a specific iteration and to reference entries of a matrix or vector. We distinguish the latter usage by using nonbold lowercase letters with a subscript (e.g. y_i corresponds to the i -th element of \mathbf{y}) when accessing elements of a vector and bold lowercase letters with two indices (or index ranges) for matrices (e.g. $\mathbf{a}_{i,:}$ corresponds to the i -th row of \mathbf{A} and $a_{i,j}$ corresponds to the entry in the i -th row and j -th column of \mathbf{A}). We define the function $\text{diag}(\mathbf{y}) : \mathbb{R}^m \mapsto \mathbb{R}^{m \times m}$, which takes an m -dimensional vector and constructs a diagonal matrix, \mathbf{D} , such that: $d_{i,j} = \begin{cases} y_i, & i = j \\ 0, & i \neq j \end{cases}$. Finally, since this work focuses on the design of distributed-memory parallel algorithms, we use bracketed superscript indices to represent matrix or vector quantities belonging to a specific processor (e.g. $\mathbf{A}^{[i]}$ or $\mathbf{y}^{[i]}$ to represent subsets of entries of \mathbf{A} or \mathbf{y} assigned to the i -th processor).

3 Optimization Problem

Given a matrix $\mathbf{A} \in \mathbb{R}^{m \times n}$ where m is the number of samples and n the number features and a vector of labels $\mathbf{y} \in \{+1, -1\}^m$, we are interested in obtaining a solution vector $\mathbf{x} \in \mathbb{R}^n$ which solves the unregularized logistic regression optimization problem:

$$f(\mathbf{A}, \mathbf{y}, \mathbf{x}) := \min_{\mathbf{x} \in \mathbb{R}^n} \frac{1}{m} \sum_{i=1}^m \log(1 + \exp(-y_i \cdot \mathbf{a}_{i,:} \cdot \mathbf{x})). \quad (1)$$

Since (1) does not have a closed-form solution, a natural way to obtain \mathbf{x} is to utilize gradient descent to iteratively compute an approximate solution \mathbf{x}_k until convergence. The gradient descent update takes the following form:

$$\mathbf{x}_k = \mathbf{x}_{k-1} - \eta \cdot \mathbf{g}_k,$$

where $\mathbf{g}_k := \nabla f(\mathbf{A}, \mathbf{y}, \mathbf{x}_{k-1})$ is the gradient with respect to the approximate solution at iteration $k - 1$ and $0 < \eta \leq 1$ is the step size (or learning rate). We only consider a fixed step size in this work. Computing the

Algorithm 1 Stochastic Gradient Descent (SGD) Algorithm to solve Equation (1)

```

1: procedure SGD( $\mathbf{A}, \mathbf{y}, \mathbf{x}_0, b, \eta, K$ )
2:   for  $k = 1, 2, \dots, K$  do
3:      $\mathbf{S}_k = \begin{bmatrix} \mathbf{e}_{i_1}^\top \\ \vdots \\ \mathbf{e}_{i_b}^\top \end{bmatrix}$  s.t.  $i_j \sim [m] \forall j = 1 \dots b$  ▷ Sample rows from  $\mathbf{I}^{m \times m}$  to construct  $\mathbf{S}_k$ 
4:      $\mathbf{u}_k = \frac{\bar{\mathbf{1}}}{\bar{\mathbf{1}} + \exp(\mathbf{S}_k \cdot \text{diag}(\mathbf{y}) \cdot \mathbf{A} \cdot \mathbf{x}_{k-1})}$  ▷ Apply the sigmoid function to a  $b$ -dimensional vector
5:      $\mathbf{g}_k = \frac{1}{b} (\mathbf{S}_k \cdot \text{diag}(\mathbf{y}) \cdot \mathbf{A})^\top \mathbf{u}_k$  ▷ Compute  $n$ -dimensional gradient w.r.t chosen samples
6:      $\mathbf{x}_k = \mathbf{x}_{k-1} - \eta \cdot \mathbf{g}_k$ 
7:   end for
8: return  $\mathbf{x}_K$ 
9: end procedure

```

gradient, \mathbf{g}_k , at each iteration requires the following quantities to be computed:

$$\mathbf{u}_k = \frac{\bar{\mathbf{1}}}{\bar{\mathbf{1}} + \exp(\text{diag}(\mathbf{y}) \cdot \mathbf{A} \cdot \mathbf{x}_{k-1})} \quad (2)$$

$$\mathbf{g}_k = \frac{1}{m} (\text{diag}(\mathbf{y}) \cdot \mathbf{A})^\top \mathbf{u}_k. \quad (3)$$

Note that $\text{diag}(\mathbf{y}) \cdot \mathbf{A}$ can be pre-computed by scaling each row (sample) of \mathbf{A} by its corresponding row (label) of \mathbf{y} . To compute \mathbf{g}_k , we must first compute \mathbf{u}_k which requires a matrix-vector product followed by nonlinear vector operations (i.e. applying the sigmoid function to an m -dimensional vector) then we can form \mathbf{g}_k by performing a (transposed) matrix-vector product. In total, using gradient descent to solve eq. (1), requires two matrix-vector operations and several linear/nonlinear vector operations on m and n dimensional vectors.

One opportunity to reduce computation in eqs. (2) and (3) is to sub-sample the rows of \mathbf{A} by pre-multiplying with a sampling matrix, $\mathbf{S}_k \in \mathbb{R}^{b \times m}$, where $b \in \mathbb{Z}^+$ *s.t.* $b < m$ is defined as a batch size. The matrix \mathbf{S}_k is constructed by sampling b rows from the m -dimensional identity matrix. This approach yields mini-batch stochastic gradient descent (SGD) shown in Algorithm 1. Note that SGD typically uses a normalization factor of $\frac{1}{b}$ instead of $\frac{1}{m}$ in the objective function. Figure 1 shows a comparison of gradient descent and SGD on the w1a (Figure 1a) and breast-cancer (Figure 1b) binary classification tasks (see Table 3) obtained from the LIBSVM repository [5]. A key difference between gradient descent and SGD is that the latter performs less computation per iteration by a factor of b/m . Therefore, we normalize the x-axis so that each iteration of gradient descent corresponds to m/b iterations of SGD. Once normalized we observed that SGD converges faster on both datasets even for convex problems (i.e. faster convergence per computation). We focus on designing efficient parallel variants of SGD motivated by these results.

4 Parallel Algorithms Design

This section surveys well-known parallelization strategies for Algorithm 1, including approaches that aim to reduce communication. We also present a novel, hybrid 2D SGD (HybridSGD) algorithm which combines existing 1D parallel variants of SGD. As Algorithm 1 illustrates, the main computation and communication bottlenecks occur in Lines 4 and 5 which require a (sparse) matrix-vector product with a $b \times n$ subsampled matrix, $\mathbf{S}_k \cdot \text{diag}(\mathbf{y}) \cdot \mathbf{A}$. In a parallel setting one or both matrix-vector products in Algorithm 1 require communication in order to form the vector quantities, \mathbf{u}_k and \mathbf{g}_k .

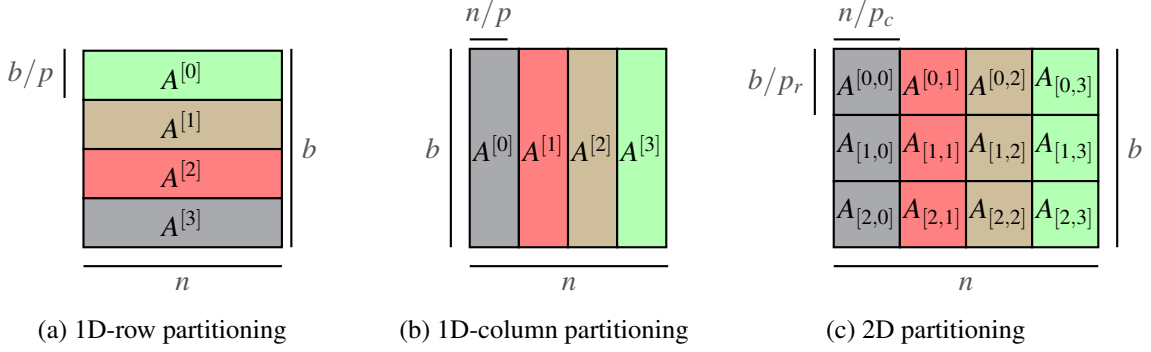


Figure 2: Various matrix partitioning strategies explored in this work. We assume that there is only enough memory to store a single copy of \mathbf{A} . While this illustrates shows partitioning strategies on dense matrices, the idea can be generalized to sparse matrices.

Figure 2 shows the data partitioning strategies used to store \mathbf{A} in distributed-memory, assuming p processors. In the 2D partitioning setting, we assume that the p processors are arranged into a 2D processor grid such that $p = p_r \times p_c$. If these partitioning schemes were applied to Algorithm 1, we can observe that under 1D-row partitioning computations involving \mathbf{A} (e.g. Line 4) requires only local matrix-vector products whereas computations with \mathbf{A}^\top (e.g. Line 5) requires local matrix-vector products as well as communication (sum-reduction) in order to form a global, n -dimensional vector, \mathbf{g}_k . Under 1D-column partitioning the reverse is true, where computations involving \mathbf{A} requires communication to form a global, b -dimensional vector, \mathbf{u}_k . 2D partitioning requires communication for both matrix-vector product computations but perform this communication on smaller b/p_r -dimensional and n/p_c -dimensional vectors. These partitioning schemes illustrate a rich performance tradeoff space for parallelizing SGD (Algorithm 1), which we will theoretically analyze in Section 5.

4.1 Communication-efficient SGD

Algorithm 2 Federated SGD with Averaging (FedAvg) Algorithm to solve Equation (1)

```

1: procedure FEDAVG( $\mathbf{A}, \mathbf{y}, \mathbf{x}_0, b, \eta, \tau, \tilde{K}$ )
2:    $\begin{bmatrix} \mathbf{A}^{[1]}, \mathbf{y}^{[1]} \\ \mathbf{A}^{[2]}, \mathbf{y}^{[2]} \\ \vdots \\ \mathbf{A}^{[p]}, \mathbf{y}^{[p]} \end{bmatrix} = \mathbf{A}, \mathbf{y}$  ▷ Partition  $\mathbf{A}, \mathbf{y}$  row-wise across  $p$  processors
3:   for  $k = 1, 2, \dots, \tilde{K}$  do
4:      $\tilde{\mathbf{x}}_k^{[i]} = \text{SGD}(\mathbf{A}^{[i]}, \mathbf{y}^{[i]}, \mathbf{x}_{k-1}, \lceil b/p \rceil, \eta, \tau)$  ▷ Compute in parallel on all processors  $i = 1, \dots, p$ 
5:      $\mathbf{x}_k = \frac{1}{p} \sum_{i=1}^p \tilde{\mathbf{x}}_k^{[i]}$ 
6:   end for
7:   return  $\mathbf{x}_K$ 
8: end procedure

```

One drawback to parallel variants of SGD is that every iteration requires communication. Therefore, if b is small, then communication becomes the performance bottleneck and barrier to scaling parallel SGD. However, there have been recent efforts in designing communication-efficient SGD variants which communicate infrequently (described in Section 2). In this work, we focus on the following two approaches:

Algorithm 3 s -step Stochastic Gradient Descent (s -step SGD) Algorithm to solve Equation (1)

```

1: procedure S-STEPSSGD( $\mathbf{A}, \mathbf{y}, \mathbf{x}_0, b, \eta, s, K$ )
2:   for  $k = 0, 1, \dots, K/s$  do
3:     for  $j = 1, 2, \dots, s$  do
4:        $\mathbf{S}_{sk+j} = \begin{bmatrix} \mathbf{e}_{i_1}^\top \\ \vdots \\ \mathbf{e}_{i_b}^\top \end{bmatrix}$  s.t.  $i_l \sim [m] \forall l = 1 \dots b$ 
5:     end for ▷ Construct  $s$  sampling matrices
6:      $\mathbf{Y} = \begin{bmatrix} \mathbf{S}_{sk+1} \\ \vdots \\ \mathbf{S}_{sk+s} \end{bmatrix} \cdot \text{diag}(\mathbf{y}) \cdot \mathbf{A}$ 
7:      $\mathbf{G} = \text{TRIL}(\mathbf{Y}\mathbf{Y}^\top)$  ▷ Compute lower-triangle of Gram matrix
8:      $\mathbf{v} = \mathbf{Y} \cdot \mathbf{x}_{sk}$  ▷ Compute partial contribution necessary to compute  $\mathbf{u}_{sk+j}$ 
9:     for  $j = 1, \dots, s$  do
10:       $\mathbf{u}_{sk+j} = [\mathbf{e}_{(j-1)b+1} | \dots | \mathbf{e}_{jb}]^\top \cdot \mathbf{v}$ 
11:      for  $l = 1, \dots, j-1$  do
12:         $\mathbf{u}_{sk+j} = \mathbf{u}_{sk+j} + \frac{\eta}{b} \cdot ([\mathbf{e}_{(j-1)b+1} | \dots | \mathbf{e}_{jb}]^\top \cdot \mathbf{G} \cdot [\mathbf{e}_{(l-1)b+1} | \dots | \mathbf{e}_{lb}]) \cdot \mathbf{u}_{sk+l}$ 
13:      end for
14:    end for ▷ Compute  $\mathbf{u}_{sk+j}$  for  $j = 1, \dots, s$  with correction due to deferred update
15:     $\mathbf{x}_{sk+s} = \mathbf{x}_{sk} - \eta \cdot \mathbf{Y}^\top \begin{bmatrix} \mathbf{u}_{sk+1} \\ \vdots \\ \mathbf{u}_{sk+s} \end{bmatrix}$  ▷ Compute solution update by combining  $s$  gradients
16:  end for
17: return  $\mathbf{x}_K$ 
18: end procedure

```

1) Federated SGD with averaging (FedAvg) [27] which combines 1D-row data partitioning with deferred communication and 2) s -step SGD [12] which combines 1D-column data partitioning with vector recurrence unrolling to reduce communication.

Algorithm 2 describes the FedAvg algorithm for solving the logistic regression problem. The algorithm begins by performing 1D-row partitioning of the input matrix (and corresponding labels) followed by iteratively calling sequential SGD (or local SGD) on each processor on only locally stored data (i.e. processor i call sequential SGD on input pairs $(\mathbf{A}^{[i]}, \mathbf{y}^{[i]})$). Each processor performs τ iterations of sequential SGD after which the resulting n -dimensional solution vector, $\tilde{\mathbf{x}}_k^{[i]}$, is communicated and averaged across all p processors. As we illustrate in Figure 4, FedAvg results in a performance-convergence tradeoff where increasing p and τ result in delayed convergence but yield faster runtimes. Note that when $p = 1$, FedAvg is equivalent to performing sequential SGD since $\tau > 1$ does not yield performance benefits. FedAvg is equivalent to sequential SGD for $p > 1$ and $\tau = 1$ provided that sequential SGD samples the same rows as FedAvg.

Algorithm 3 describes the s -step SGD algorithm for solving the logistic regression problem. The algorithm was first presented in [12], which showed that communication can be deferred for s iterations without affecting convergence behavior of SGD. In contrast to FedAvg, s -step SGD introduces a computation-communication tradeoff where communication is avoided for s iterations but requires more computation and communication volume (i.e. message sizes increase proportional to s). This additional computation arises in Line 7, where a Gram matrix (\mathbf{G}) is formed and whose blocks are used in Line 9–Line 13 to perform corrections on \mathbf{u}_{sk+j} due to deferred updates on the solution vector. A natural way to parallelize Algorithm 3

Algorithm	Flops (F)	Convergence rate	Storage (M)
1D-row SGD	$K \cdot \left(\frac{bc}{p} + n\right)$	$1/(Kb)$	$cm/p + n$
1D-column SGD	$K \cdot \left(\frac{bc}{p} + n/p\right)$	$1/(Kb)$	$cm/p + b + n/p$
2D SGD	$K \cdot \left(\frac{bc}{p} + n/p_c\right)$	$1/(Kb)$	$cm/p + b/p_r + n/p_c$
s-step SGD	$(K/s) \cdot \left(\frac{c^2 \binom{s}{2} b^2}{n \cdot p} + \binom{s}{2} b^2 + n/p\right)$	$1/(Kb)$	$cm/p + \binom{s}{2} b^2 + n/p$
FedAvg	$\tilde{K} \cdot \tau \cdot \left(\frac{bc}{p} + n\right)$	$1/(\tilde{K}bp)$, if $\tau = O\left(\sqrt{\tilde{K}/(bp)}\right)$	$cm/p + n$
HybridSGD	$(\hat{K}/s) \cdot \left(\frac{c^2 \binom{s}{2} b^2}{n \cdot p \cdot p_r} + \binom{s}{2} \frac{b^2}{p_r^2} + \tau \cdot n/p_c\right)$	$1/(\hat{K}bp_r)$, if $\tau = O\left(\sqrt{\hat{K}/(bp_r)}\right)$	$cm/p + \binom{s}{2} \frac{b^2}{p_r^2} + n/p_c$

Table 1: Theoretical flops, convergence rates, and storage costs of parallel SGD variants, FedAvg, s -step SGD, and HybridSGD. HybridSGD uses a 2D processor grid such that $p = p_r \times p_c$. We assume that each row of \mathbf{A} contains $c > 0$ nonzeros and the entire matrix contains cm total nonzeros. We also assume that the nonzeros are uniformly distributed such that all data partitioning schemes yield load balanced processors (i.e. each processor stores at least $M = cm/p$) nonzeros. All costs are to leading-order. Algorithms shown in **bold** represent communication-efficient variants of SGD.

requires \mathbf{A} to be 1D-column partitioned, so that Line 7 requires a reduction operation to form \mathbf{G} . Any other partitioning scheme results in additional communication in the form of a parallel 1D or 2D matrix multiplication to form the Gram matrix and to perform the computations in Line 9–Line 13. Therefore, 1D-column partitioning yields the cheapest overall communication cost when parallelizing Algorithm 3.

HybridSGD Design. Given that FedAvg and s -step SGD are both reduce communication cost of SGD using different 1D data partitioning layouts, we propose to combine both and develop a 2D, parallel hybrid SGD (HybridSGD) algorithm. HybridSGD leverages 2D data partitioning such that processors spanning rows perform FedAvg (on n/p_c fractions of \mathbf{x}) and processors spanning columns perform s -step SGD on b/p_r independent batches of rows of \mathbf{A} . Note that the algorithm for HybridSGD can be obtained by augmenting Algorithm 2, such that \mathbf{A} is column and row partitioned and where Line 4 is replaced with a call to Algorithm 3. A key difference between HybridSGD and s -step SGD is that the condition $s \leq \tau$ must hold for HybridSGD since Algorithm 3 is performed for at most τ iterations before the local solution vectors, $\tilde{\mathbf{x}}_k^{[i]}$, are communicated and averaged.

5 Algorithms Analysis

Tables 1 and 2 summarize the theoretical costs of parallel SGD (1D and 2D partitioning of \mathbf{A}) and communication efficient SGD variants (s -step SGD, FedAvg, and HybridSGD), which we prove in this section. We assume that the sparse matrix, $\mathbf{A} \in \mathbb{R}^{m \times n}$, contains $c > 0$ nonzeros per row. We assume that the nonzeros are uniformly distributed such that the partitioning of \mathbf{A} across p processors is load balanced (i.e. each processor contains cm/p nonzeros). Since we work with variants of (mini-batch) SGD which selects b rows of \mathbf{A} at every iteration, the total number of nonzeros is given by bc with each processor assumed to store bc/p nonzeros. This nonzero distribution yields probabilistic flops bounds, particularly for s -step SGD and HybridSGD which rely on a 1D-parallel sparse, symmetric rank-k update (SYRK) computation. We prove asymptotic bounds on the computation, convergence, communication, and storage requirements of the algorithms studied in this work.

We assume that \mathbf{A} is stored in compressed sparse row (CSR) format, so that subsampling rows at each

iteration can be performed easily by constructing a new row-index array. Due to performance considerations, we subsample rows of \mathbf{A} cyclically (using the function $i = (i + b) \bmod m$). We also pad \mathbf{A} with additional rows to ensure that $0 \equiv m \bmod (s_{\max} \cdot b)$, where s_{\max} corresponds to the largest value of s in a given experiment.

5.1 Computation, Convergence, and Storage

We model the cost of an algorithm as the sum of computation time and communication time, where computation time is defined as follows,

$$T_{\text{comp}} = \gamma \cdot F,$$

where F is the number of floating-point operations performed by the algorithm and γ (units of seconds per floating-point operation) corresponds to how fast a candidate CPU can perform (floating-point) computations. This section will prove computation and storage cost bounds for the SGD variants proposed in this work. A summary of the computation, convergence, and storage costs are shown in Table 1. Proofs of convergence rate for SGD, s -step SGD, and FedAvg are well-known, so we state convergence rates and provide references for interested readers in Table 1 and in Section 5.3.

Theorem 5.1.1. *K iterations of SGD with \mathbf{A} distributed across a 2D processor grid (2D SGD) of size $p = p_r \times p_c$ processor must perform $F = O(K \cdot (\frac{bc}{p} + n))$ flops and store $M = O(cm/p + n)$ words in memory per iteration.*

Proof. We prove the computation cost by analyzing Algorithm 1 under the assumption that \mathbf{A} is distributed across a 2D processor grid and where b -dimensional vector quantities are distributed across the p_r processor dimension and n -dimensional vector quantities are distributed across the p_c processor dimension. Under this setting, forming \mathbf{u}_k requires a parallel sparse matrix vector product (SpMV) between $\mathbf{S}_k \cdot \text{diag}(\mathbf{y}) \cdot \mathbf{A} \cdot \mathbf{x}_{k-1}$. Note that sampling b/p_r rows of \mathbf{A} on each processor row team requires constructing a new CSR row-pointer array of length b/p_r . Scaling each row of the subsampled matrix requires work proportional to the number of nonzeros, which costs bc/p flops due to the uniform nonzero distribution assumption. Once $\mathbf{S}_k \cdot \text{diag}(\mathbf{y}) \cdot \mathbf{A}$ is constructed the parallel SpMV costs bc/p . This is obtained by considering that each row team operates on b/p_r rows of the sampled matrix such that each column team contains c/p_c nonzeros per row (in expectation). Multiplying these quantities yields bc/p flops for the parallel SpMV, in expectation. Each processor row team stores the output vector (of dimension b/p_r) and performs nonlinear operations to form \mathbf{u}_k , which costs $\phi b/p_r$, where $\phi > 1$ is a constant which accounts for the increased computational cost of performing the $\exp(\cdot)$ and division operations. The next operation is a second parallel SpMV which costs bc/p flops, as before. Finally, updating \mathbf{x}_k requires $2n/p_c$ flops. Summing these costs, multiplying by the total number of SGD iterations (K), and dropping lower-order terms yields the results stated in Theorem 5.1.1. The storage costs can be obtained from the computation cost analysis by noting that \mathbf{A} contains cm total nonzeros all of which are uniformly distributed and partitioned across p processors (where $p = p_r \times p_c$). This results in storage cost of cm/p per processor to store a single copy of \mathbf{A} . Each row team requires additional memory to store b/p_r -dimensional and n/p_c -dimensional (dense) subvectors corresponding to \mathbf{u}_k and \mathbf{g}_k , respectively. Summing these costs proves the storage bound. \square

The computation and storage bounds for 2D SGD shown in Theorem 5.1.1 can be specialized to 1D-row and 1D-column partitioned SGD by setting $p_c = 1$ or $p_r = 1$ (and dropping lower-order terms), respectively.

Theorem 5.1.2. *\tilde{K} iterations of FedAvg with \mathbf{A} distributed across p processors in 1D-row layout must perform $F = O(\tilde{K} \cdot \tau \cdot (bc/p + n))$ flops and store $M = O(cm/p + n)$ words in memory per iteration.*

Proof. From Algorithm 2 we can observe that each processor stored m/p rows of \mathbf{A} locally, which requires cm/p words of memory since each row contains c nonzeros. Since b represents that global batch size, each

processor selects b/p local rows and performs τ iterations of sequential SGD. Each iteration of sequential SGD requires bc/p flops due to the SpMV and n flops to update $\tilde{\mathbf{x}}_k^{[i]}$ on each processor. A total of $\tau \cdot (bc/p + n)$ flops are required per sequential SGD call (i.e. Line 4) and a total of $\tilde{K} \cdot \tau \cdot (bc/p + n)$ flops for FedAvg to leading-order. Since each processor stored cm/p nonzeros of \mathbf{A} and requires a local solution vector, the storage costs per processor are $cm/p + n$ to leading-order. \square

Theorem 5.1.3. \hat{K} iterations of HybridSGD with \mathbf{A} distributed across a 2D processor grid of size $p = p_r \times p_c$ processors must perform $O\left(\left(\hat{K}/s\right) \cdot \left(\frac{c^2 \binom{s}{2} b^2}{n \cdot p \cdot p_r} + \binom{s}{2} \frac{b^2}{p_r^2} + \tau \cdot n/p_c\right)\right)$ flops and store $M = O\left(cm/p + \binom{s}{2} \frac{b^2}{p_r^2} + n/p_c\right)$ words in memory per iteration.

Proof. HybridSGD is a 2D variant of FedAvg (1D-row layout) where Line 4 in Algorithm 2 is replaced with a call to parallel s -step SGD (1D-column layout). Assuming a global batch size of b , each processor row team is assigned a local batch size of b/p_r . Substituting b/p_r into the flops cost of s -step SGD in Table 1 yields the cost of performing s -step SGD. After each s -step SGD call, the solution vector (of dimension- n/p_c) must be updated. This update occurs \hat{K} times in total. However, if $s < \tau$, then the solution vector is updated after s iterations of s -step SGD, so τ/s solution updates are required per s -step SGD call. An additional solution update is required after the s -step SGD call to compute the global solution. Multiplying these costs by the total number of HybridSGD iterations, \hat{K} , yields the stated computation cost. The storage cost of HybridSGD can be obtained directly from the s -step SGD storage cost in Table 1, by setting $b = b/p_r$ and replacing n/p with n/p_c . \square

The results of Theorems 5.1.1 to 5.1.3 suggests that parallel SGD (1D and 2D variants) and FedAvg have comparable computation and storage costs, whereas s -step SGD and HybridSGD increase both costs. In order for FedAvg to perform better than parallel SGD the condition $\tilde{K} < K/\tau$ must hold. Since FedAvg attains a linear speedup in convergence rate as p increases, allowing $p \geq \tau$ enables FedAvg to converge faster than parallel SGD. Note that b is defined as the global batch size for ease of comparison between the various SGD variants analyzed. In practice, b is a hyperparameter which can be varied independently for each algorithm. We exploit this in Section 6 while studying the performance tradeoffs of s -step SGD, FedAvg, and HybridSGD.

5.2 Communication

In the parallel setting (especially in the distributed-memory parallel setting) the cost of interprocessor communication can be just as expensive (and possibly more so) than computation. In this section, we prove bounds the cost of communication for parallel variants of SGD. We use Hockney’s $(\alpha - \beta)$ performance model which approximates communication time using the following equation:

$$T_{\text{comm}} = \alpha \cdot L + \beta \cdot W,$$

where L is the number of messages required to synchronize/communicate across p processors and W is the number of words communicated per synchronization/communication event (e.g. point-to-point or collective operations). The parameters α (units of seconds per message) and β (units of seconds per word moved) correspond to hardware costs, which depend on the distributed-memory communication library (e.g. MPI and the underlying network routing algorithm) and hardware features (e.g. network bandwidth, communication channels, and NIC). Table 2 summarizes the communication cost of the SGD variants we study under Hockney’s two-term communication model. We assume throughout that Algorithms 1 to 3 use an MPI allreduce collective in order to communicate. We further assume that the cost of allreduce can be modeled by $L = 2 \cdot \log(p)$ and $W = d$, where d is the message size (in words moved). These bounds on message size

Algorithm	Bandwidth (W)	Latency (L)
1D-row SGD	$K \cdot b$	$K \cdot \log p$
1D-column SGD	$K \cdot n$	$K \cdot \log p$
2D SGD	$K \cdot (b/p_r + n/p_c)$	$K \cdot (\log p_r + \log p_c)$
s-step SGD	$(K/s) \cdot \binom{s}{2} b^2$	$(K/s) \cdot \log p$
FedAvg	$\tilde{K} \cdot n$	$\tilde{K} \cdot \log p$
HybridSGD	$(\hat{K}/s) \cdot \binom{s}{2} b^2/p_r^2 + \hat{K} \cdot n/p_c$	$\hat{K} \cdot \log p_r + (\hat{K}/s) \cdot \log p_c$

Table 2: Theoretical parallel communication costs of parallel SGD variants, FedAvg, s -step SGD, and HybridSGD using Hockney’s two-term communication model (bandwidth and latency). HybridSGD uses a 2D processor grid such that $p = p_r \times p_c$. For the cost analysis, we assume that quantities being communicated are stored as dense vectors. All costs are to leading-order. Algorithms shown in **bold** represent communication-efficient variants of SGD.

and latency are attained through the use of a reduce-scatter followed by an allgather [28, 22]. Algorithms 1 and 3 utilize an allreduce communication step in order to sum-reduce partial vectors (of dimension b or n depending on layout) during gradient computation. The computations following communication to aggregate the gradient vector are performed redundantly on all processors (i.e. these computations are inherently sequential). We prove asymptotic bounds on total bandwidth and total latency (to leading-order) below. Asymptotic bounds per-iteration can be obtained by eliminating all terms involving K, \hat{K}, \tilde{K} in Table 2. We prove bounds for 2D SGD and show how to specialize the bounds to 1D-column or 1D-row SGD. We refer readers to [12] for proof of s -step SGD, which are summarized in Tables 1 and 2.

Theorem 5.2.1. K iterations of SGD with \mathbf{A} distributed across a 2D processor grid (2D SGD) of size $p = p_r \times p_c$ processors must communicate $W = O(Kb/p_r + Kn/p_c)$ words using $L = O(K \log p_r + K \log p_c)$ messages.

Proof. From Algorithm 1 we can observe that allreduce communication is required only in Lines 4 and 5. Sampling can be coordinated by ensuring that all processors along the row dimension (in Figure 2c) are initialized to the same random number generator and seed. Once the gradient, \mathbf{g}_k , is computed all processors along the column dimension redundantly store n/p_c subvectors of \mathbf{g}_k and \mathbf{x}_k . Therefore, updating \mathbf{x}_k also requires no communication. Forming \mathbf{u}_k requires allreducing a b/p_r -dimensional subvector simultaneously along each processor row, which requires communicating b/p_r words using $\log p_c$ messages, assuming that processors teams in different rows can communicate simultaneously without contention. A similar argument gives n/p_c words and $\log p_r$ messages to form \mathbf{g}_k . Multiplying each cost by K iterations and summing yields the results of Theorem 5.2.1. Setting $p_c = 1$ or $p_r = 1$ yields the bounds for 1D-row SGD and 1D-column SGD, respectively, stated in Table 2. \square

Theorem 5.2.2. \tilde{K} iterations of FedAvg with \mathbf{A} distributed across p processors in 1D-row layout must communicate $W = O(\tilde{K} \cdot n)$ words using $L = O(\tilde{K} \cdot \log p)$ messages.

Proof. Once \mathbf{A} is 1D-row partitioned, each processor performs τ local iterations of sequential SGD before communicating $\mathbf{x}_k^{[i]}$, the local solution on processor i , via an allreduce. This requires n words to be moved (since $\mathbf{x}_k^{[i]} \in \mathbb{R}^n$) using $\log p$ messages. The frequency of communication is \tilde{K} , since an allreduce is required after Line 4 in Algorithm 2. Multiplying each cost by the number of calls proves Theorem 5.2.2. \square

While there are similarities in the communication costs between Theorem 5.2.2 and Theorem 5.2.1 ($p_c = 1$, 1D-row SGD variant), the bounds differ in the number of iterations for each algorithm. If we

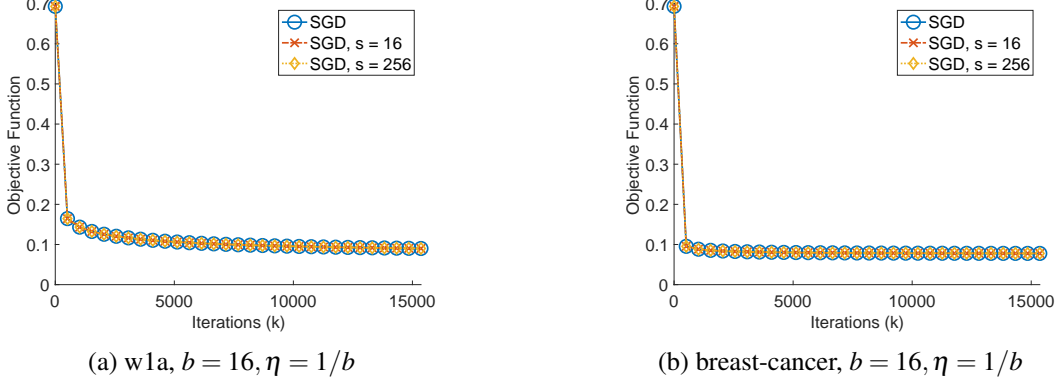


Figure 3: Convergence behavior of s -step SGD for a fixed batch size ($b = 16$), fixed learning rate ($\eta = 1$), and varying values of s on the w1a and breast-cancer datasets. The maximum entry-wise error in the s -step solution was on the order of 10^{-14} (Figure 3a) and 10^{-15} (Figure 3b) when compared to the SGD solution.

assume that FedAvg and 1D-row SGD converge at the same rate, then $K = \hat{K} \cdot p$, as FedAvg allows for linear speedup in convergence as the number of processors is increased (provided that τ is bounded).

Theorem 5.2.3. \hat{K} iterations of HybridSGD with \mathbf{A} distributed across a 2D processor grid of size $p = p_r \times p_c$ processors must communicate $W = O\left(\hat{K}/s \cdot \frac{\binom{s}{2} b^2}{p_r^2} + \hat{K}/\tau \cdot \frac{n}{p_c}\right)$ words using $L = O(\hat{K}/\tau \cdot \log p_r + \hat{K}/s \cdot \log p_c)$ messages.

Proof. In order to make communication costs comparable across algorithms, we assume that HybridSGD uses a batch size of b/p_r , where b is the global batch size. From [12] we know that s -step SGD requires $K/s \cdot \binom{s}{2} b^2$ words to be moved using $K/s \cdot \log p$. In HybridSGD, each of the p_r processor row teams perform s -step SGD on a batch of b/p_r samples from locally stored rows of \mathbf{A} using p_c processors per row team. The s -step SGD costs can be specialized by updating the batch size and processors. This results in each processor row team communicating $\binom{s}{2} b^2 / p_r^2$ words using $\log p_c$ messages. Each of the p_c processor columns performs FedAvg on an n/p_c -dimensional subvector of $\tilde{\mathbf{x}}_k^{[i]}$, where i is a processor column index. By specializing Theorem 5.2.2 to the number of processors in each column (i.e. p_r) and solution vector size (n/p_c), we obtain a communication cost of n/p_c words moved using $\log p_r$ messages. If we assume \hat{K} iterations of HybridSGD are required, then FedAvg requires \hat{K}/τ rounds of communication. HybridSGD replaces the local SGD call within FedAvg (Line 4 in Algorithm 2) with calls to parallel s -step SGD (Algorithm 3) with $K = \tau$ and using p_c processors. So, parallel s -step SGD requires τ/s allreduce calls. Since s -step SGD is called a total of \hat{K}/τ times, the total number of allreduce calls for parallel s -step SGD is \hat{K}/s . The results of Theorem 5.2.3 can now be obtained by multiplying FedAvg communication cost by \hat{K}/τ and multiplying parallel s -step SGD communication cost by \hat{K}/s . \square

5.3 Convergence

Figure 3 shows the convergence behavior (in terms of the objective function) of SGD and s -step SGD for $s \in \{16, 256\}$ on the w1a (Figure 3a) and breast-cancer (Figure 3b) datasets with a fixed batch size ($b = 16$) and learning rate ($\eta = 1$). Since Algorithm 3 is an algebraic reformulation of Algorithm 1, the solution is expected to be mathematically equivalent, up to floating-point error. The convergence of FedAvg are shown in Figure 4 on the w1a and breast-cancer datasets for a fixed learning rate ($\eta = 1$ and $\eta = 0.5$), batch size ($b = 16$), and delay ($\tau = 100$), while p is varied (note that $p_r = p$ for FedAvg). As p is increased, the convergence of FedAvg slows due to approximation error, since FedAvg assumes that the global solution is

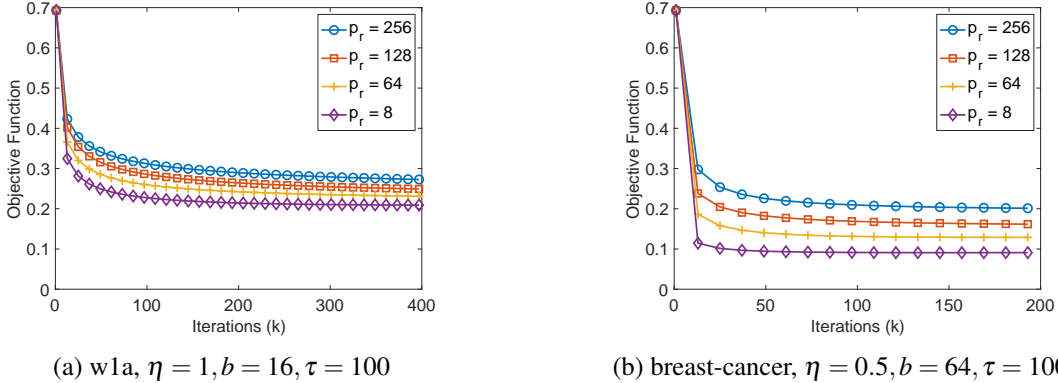


Figure 4: Convergence behavior of FedAvg for a fixed batch size (b) and aggregation delay (τ) on the w1a and breast-cancer dataset for various values of p_r . For FedAvg $p_r = p$. Learning rate (η) was tuned to ensure convergence.

Name	m	n	Sparsity (%)
w1a	2477	300	96.18%
breast-cancer	683	10	0%
url	2396130	3231961	99.99%
epsilon	400000	2000	0%

Table 3: A summary of the datasets used in the convergence and performance experiments presented in this paper. All datasets are binary classification tasks obtained from the LIBSVM repository [5]. We chose small-scale datasets for MATLAB (convergence) experiments and large-scale datasets for parallel experiments.

the average of p local solutions. The approximation error can be decreased by selecting a small value for τ at the expense of parallel performance. Figure 4b shows similar behavior for the breast-cancer dataset. The convergence behavior implies that $p_r = 1$ is best to obtain fast convergence, but $p > 1$ may decrease the running time sufficiently to overcome the convergence delay introduced for $\tau > 1$.

As the convergence results indicate, s -step SGD creates a computation-bandwidth-latency tradeoff as a function of s and FedAvg creates a convergence-performance tradeoff as a function of p and τ . Through the use of a 2D processor grid ($p = p_r \times p_c$) HybridSGD enables a continues tradeoff between s -step SGD and FedAvg. As Table 1 shows, HybridSGD reduces the computation and bandwidth cost of s -step SGD by a factor of p_r^2 at the expense a slower convergence rate due to the use of FedAvg along the processor row dimension (p_r). Since HybridSGD uses a 2D processor grid ($p = p_r \times p_c$), its convergence is expected to be faster than FedAvg when $p_c > 1$. In contrast to FedAvg, HybridSGD allows one to select a particular convergence curve (i.e. a specific value of p_r) and continue to increase parallelism (i.e. decrease running time) by increasing p_c . An additional benefit is that the bandwidth cost of communicating across the processor row teams (p_r dimension) is decreased by a factor of p_c in comparison to FedAvg (see Table 2). The communication cost of HybridSGD is complicated by the additional bandwidth cost of communicating across the p_c dimension. This additional bandwidth cost can be mitigated since s, b, p_r , and p_c are all tunable hyperparameters, whereas n depends on \mathbf{A} .

6 Experiments

We implement the SGD variants described in Section 4 in C++ using the Message Passing Interface [15] for parallel processing (Cray MPICH 8.1.28). We use the Intel oneAPI MKL [17] library (Intel oneAPI 2023.2.0) for dense and sparse BLAS routines. All experiments were performed on the NERSC Perlmutter (Cray EX supercomputer) [20] using the CPU-only partition. We experimented with using a mixed OpenMP+MPI programming model, but found that shared-memory parallelism did not yield performance improvements. Therefore, we use flat-MPI for all performance studies presented in this section. Due to performance considerations, we construct \mathbf{S}_k by subsampling rows cyclically instead of stochastically. If $m \bmod b \neq 0$, then we pad the sampled matrix with zeroes to ensure that \mathbf{u}_k is always b -dimensional. \mathbf{A} is stored in the three-array compressed sparse row (CSR) format using an MKL sparse matrix handle. We explicitly create a new MKL sparse matrix handle in each iteration of SGD (any variant) since computations are performed with a batch of b rows of \mathbf{A} . We destroy the MKL sparse matrix handle after use to ensure that the memory footprint of each SGD variant is minimized over the lifetime of the algorithm. We performed offline tests where we explicitly create a length- m/b array of MKL sparse matrix handles (representing all cyclic batches) to take advantage of MKL’s nonzero reordering methods, but found that this approach did not yield speedups. All experiments are performed in single-precision with floating-point memory buffers aligned to 64-byte boundaries. We implement a custom timer class which uses the C++14 chrono library. This implementation adds a runtime overhead of 15% to 20% depending on the SGD variant (e.g. s -step SGD and HybridSGD require more timers in inner loops). Finally, we use binary classification datasets obtained from the LIBSVM repository [5]. Table 3 summarizes the datasets used in the sequential experiments (in Section 5.3) and the parallel experiments.

6.1 Convergence vs. Runtime

Figure 5 shows a comparison of the convergence behavior of s -step SGD and HybridSGD to a fixed objective value on the url and epsilon datasets. We report the convergence behavior in terms of the number of gradient evaluations (Figures 5a and 5c) and in terms of running time (Figures 5b and 5d). We performed grid search on the values of s for both algorithms, as well as, the 2D processor grid dimensions for HybridSGD. Finally, we report results with respect to hyperparameters settings which attained the best running time for each algorithm. The left y-axis depicts the loss function value and the right y-axis shows the training accuracy.

Figures 5a and 5b illustrate the convergence for the url dataset. These results show that HybridSGD requires a factor of $15\times$ more gradient evaluations than s -step SGD in order to converge to the same objective value due to the delay in convergence from incorporating FedAvg. However, when the x -axis is normalized to runtime (in Figure 5b), we see that HybridSGD converges faster by a factor of $5.3\times$ since one iteration of HybridSGD is faster than one iteration of s -step SGD.

Figures 5c and 5d show the convergence for the dense, epsilon dataset. Since the epsilon dataset is over-determined, each of $p_r = 4$ row teams that perform s -step SGD contain 100,000 rows of \mathbf{A} per team. Furthermore, the rank of $\mathbf{A}^T\mathbf{A}$ is at most $n = 2000$. Given these constraints, FedAvg can perform a large number of local iterations (i.e. $\tau = 8192$ in these experiments) before communicating. Another consequence is that the epsilon dataset exhibits no convergence delay due to the use of HybridSGD with $p_r > 1$. As with the url dataset, normalizing the x -axis to gradient evaluations illustrates that HybridSGD must perform more work than s -step SGD. However, once normalized with respect to runtime, HybridSGD becomes the faster of the two algorithms (by a modest factor of $1.15\times$). Overall, these experiments indicate that HybridSGD requires more gradient evaluations than s -step SGD (the fastest SGD variant), but each gradient evaluation is cheaper than s -step SGD (and sufficiently cheaper to overcome convergence delays).

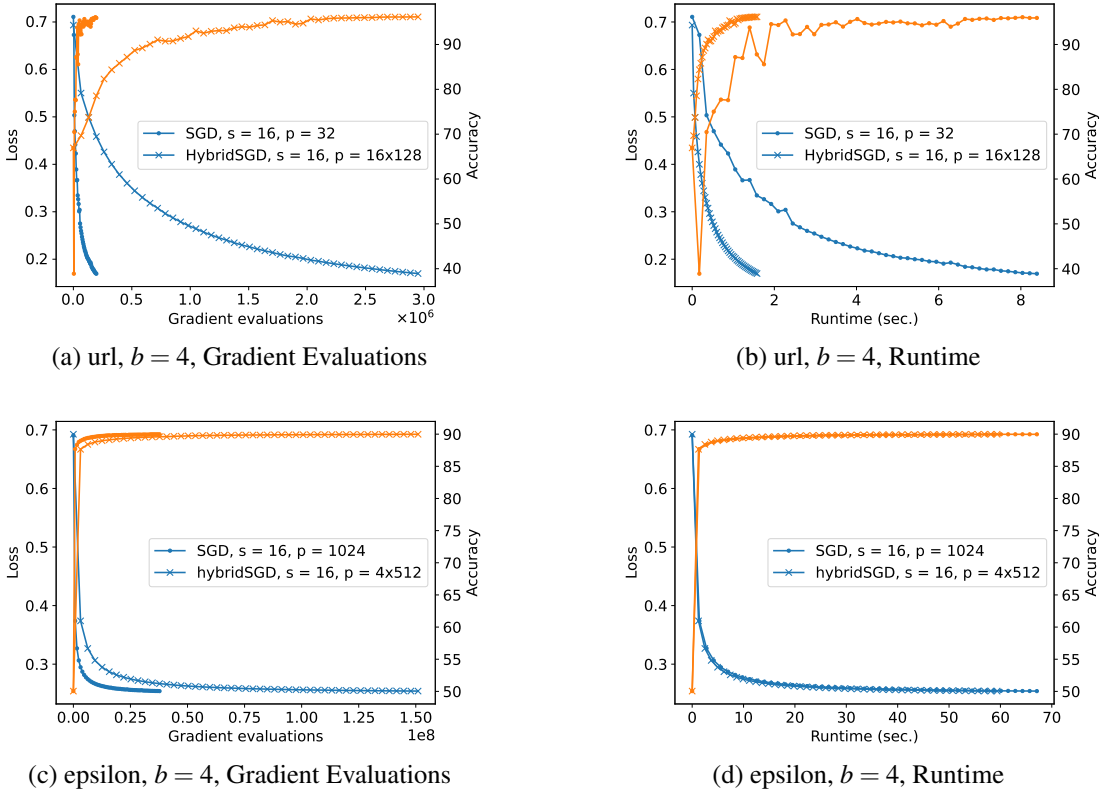


Figure 5: Comparison of convergence behavior and accuracy of s -step SGD and HybridSGD at small batch sizes ($b = 4$) after offline tuning of s on the url dataset (sparse). We show convergence in terms of the number of gradient evaluations (Figure 5a) and the running time (Figure 5b).

6.2 Strong Scaling Performance

The HybridSGD algorithm creates a continuous tradeoff between FedAvg and s -step SGD through the use of a 2D processor grid where FedAvg is performed with p_r processors such that each SGD call within FedAvg is replaced with a parallel s -step SGD call that are parallelized across p_c processors. Each s -step SGD call operates on an m/p_r fraction of rows of \mathbf{A} . Therefore, HybridSGD is a generalization of the two approaches such that FedAvg can be recovered by setting $p_c = 1$ and s -step SGD can be recovered by setting $p_r = 1$. In this section we study the scaling performance of HybridSGD in comparison to s -step SGD under the large batch size and small batch size settings. The large batch size setting aims to study whether HybridSGD provides speedups and/or better scalability over classical parallel SGD (i.e. the batch size is too large for s -step SGD to be practical). The small batch size setting aims to study strong scaling behavior in the regime where s -step SGD with $s > 1$ is possible.

Large Batch Sizes. Figure 6 shows the strong scaling behavior of parallel SGD (1D-column data layout) in comparison to HybridSGD (2D data layout) on the url (sparse) and epsilon (dense) datasets obtained from the LIBSVM repository. We perform offline tuning on the grid size for HybridSGD for a given processor count and report the grid size which achieved the best runtime.

In Figure 6a, parallel SGD exhibits poor scaling behavior due to load imbalance. The url dataset has non-uniform nonzero distribution where a few rows in the matrix contain a majority of the nonzeros. Since parallel SGD uses a 1D-column data layout, the load imbalance cannot be fixed. For example, with $p < 16$,

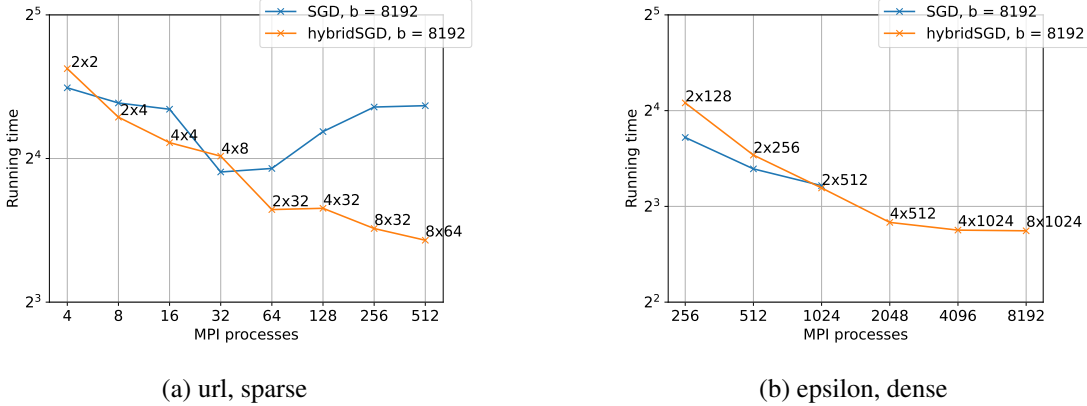


Figure 6: Strong scaling comparison of SGD and HybridSGD for the large batch size setting ($b = 8192$) on a sparse (Figure 6a) and dense (Figure 6b) input matrices.

MPI processor rank 0 contains 96% of the nonzeros in the matrix. Therefore, most of the running time is spent waiting for rank 0 to communicate results of its local SpMV. Once p is increased (e.g. $32 \leq p \leq 512$), the load imbalance decreases sufficiently to yield runtime improvements. We observed that once $p = 32$ the number of nonzeros on MPI rank 0 reduces to 54% of the total nonzeros. This reduction in nonzeros yields a runtime speedup of $1.35\times$ at $p = 32$ when compared to the runtime at $p = 16$. HybridSGD leverages a 2D data layout which partitions the rows and columns of the input matrix. Figure 6a highlights the performance improvements obtained by introducing row partitioning in HybridSGD. For example, we see better scaling behavior for $p \leq 32$ and faster runtimes for $p \geq 64$. For the url dataset, a 2D layout allows the column dimension (i.e. using SGD) to operate at its fastest processor count ($16 \leq p \leq 32$) and allows scalability (beyond $p = 32$) via the row dimension (i.e. using FedAvg).

Figure 6b shows the strong scaling behavior on the dense, epsilon dataset, where parallel SGD is nearly load balanced (up to $n \bmod p$ ranks store one extra column). Due to better load balance, parallel SGD exhibits better scaling behavior but cannot scale beyond $p = 1024$ since $n = 2000$. Since HybridSGD uses a 2D processor grid, we can leverage row partitioning to achieve more parallelism while ensuring $p_{col} < n$. Note that at $p = 256$ and $p = 512$ HybridSGD is slower than SGD for two reasons. First, HybridSGD must overcome delayed convergence due to FedAvg. Second, HybridSGD communicates messages of size $n/p_{row} + b$ whereas SGD communicates messages of size b . When p is small, we expect HybridSGD to be slower than SGD. Once SGD reaches its scaling limit, HybridSGD becomes faster as the reduction tree in the column dimension (SGD) becomes shorter (by a factor of $2\times$) and the row dimension (FedAvg) communicates infrequently (every τ iterations). For the epsilon dataset, using HybridSGD results in $2\times$ more scalability. HybridSGD achieved speedups of $1.39\times$ on both datasets over parallel SGD (speedups are relative to the fastest parallel SGD runtime).

FedAvg must compute the global average over p local weight vectors (of dimension n). As a result, the runtime of FedAvg is dominated by the cost of performing computation on and communicating n -dimensional vectors. Since FedAvg uses 1D row partitioning on A , the batch size range is limited to $1 \leq b \leq \lceil m/p \rceil$. This batch size limitation also impacts the choice of τ . Once τ exceeds $\lceil \frac{m}{p \cdot b} \rceil$, the value of continuing local optimization decreases [27]. HybridSGD, in contrast, reduces p in FedAvg to p_r which facilitates larger values of τ without affecting convergence. HybridSGD attained speedups of $121\times$ on url and $72\times$ on epsilon over FedAvg (we used $p = 512$ on url and $p = 2048$ on epsilon). This suggests that when n is sufficiently large, HybridSGD is always faster than FedAvg.

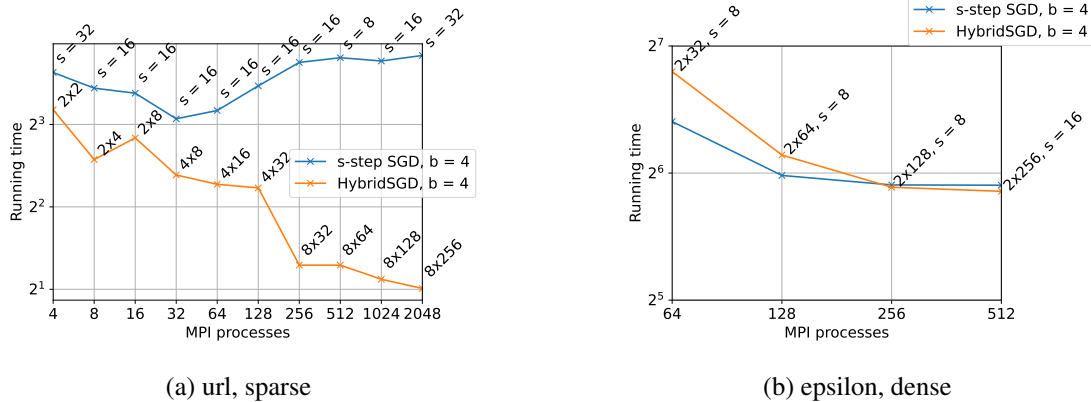


Figure 7: Strong scaling comparison of s -step SGD and HybridSGD for the small batch size setting ($b = 4$) on a sparse (Figure 7a) and dense (Figure 7b) input matrix.

Small Batch Sizes. Figure 7 shows the strong scaling behavior of s -step SGD and HybridSGD with $b = 4$ on the url (sparse) and epsilon (dense) datasets. We perform offline tuning on processor grid dimensions for HybridSGD and on the value of s for both algorithms and report the setting corresponding to the best runtime to achieve a target objective value/training accuracy.

In Figure 7a, we see that s -step SGD does not exhibit good scalability due to the load-imbalance issue identified in Figure 6a. However, HybridSGD is once again able to achieve better scaling than s -step SGD. We observed that $s = 32$ was the best choice at $p = 4$ and $p = 8$, while $s = 16$ was best for $p > 8$. HybridSGD achieved a $5.3\times$ speedup at $p = 2048$ over s -step SGD at $p = 32$. Similar to the large batch setting, increasing the processor count for s -step SGD does not yield any speedups as finer column partitioning (assigns n/p columns per processor) does not alleviate load imbalance. In contrast, HybridSGD can increase p_r (assigns m/p_r rows per processor) apply finer partitioning to the rows in order to overcome load balancing issues. We note that HybridSGD achieves a large speedup of $1.92\times$ when scaling from $p = 128$ to $p = 256$, by increasing p_r while keeping p_c fixed. We observed a $1.99\times$ decrease in the number of nonzeros assigned to rank 0 when shifting from a grid size of $(p_r = 4, p_c = 32)$ to a grid size of $(p_r = 8, p_c = 32)$.

In Figure 7b, we show HybridSGD performance in comparison to s -step SGD in the small batch size regime. Note that due to the similar scaling curves, we omit annotations for s -step SGD. The values of s for s -step SGD are the same as those annotated for HybridSGD except at $p = 256$, where s -step SGD achieved the shown runtime with a value of $s = 16$. Unlike in the large batch size setting, we see that HybridSGD achieves only a slight speedup over s -step SGD at the scaling limit of $p = 512$. At such small batch sizes both algorithms are memory-bandwidth bound (since the epsilon dataset is dense), so HybridSGD is unable to significantly improve upon the s -step SGD performance. Note, however, that when the algorithm becomes communication bound at large batch sizes (see Figure 6b), HybridSGD clearly outperforms s -step SGD for the epsilon dataset.

6.3 Running Time Breakdown

Figure 8 shows the running time breakdown of s -step SGD in comparison to HybridSGD for a fixed number of processors. We report the breakdown as the fraction of runtime spent on a particular computation or communication event (e.g. SpMV and s -step communication). Since each processor maintains timers, we take the max timer for each timing category over all processors. Timing categories which comprise less than 5% of the runtime are gathered into the 'other time' category.

In Figure 8a we show the timing breakdown for the sparse, url dataset. We performed offline tuning

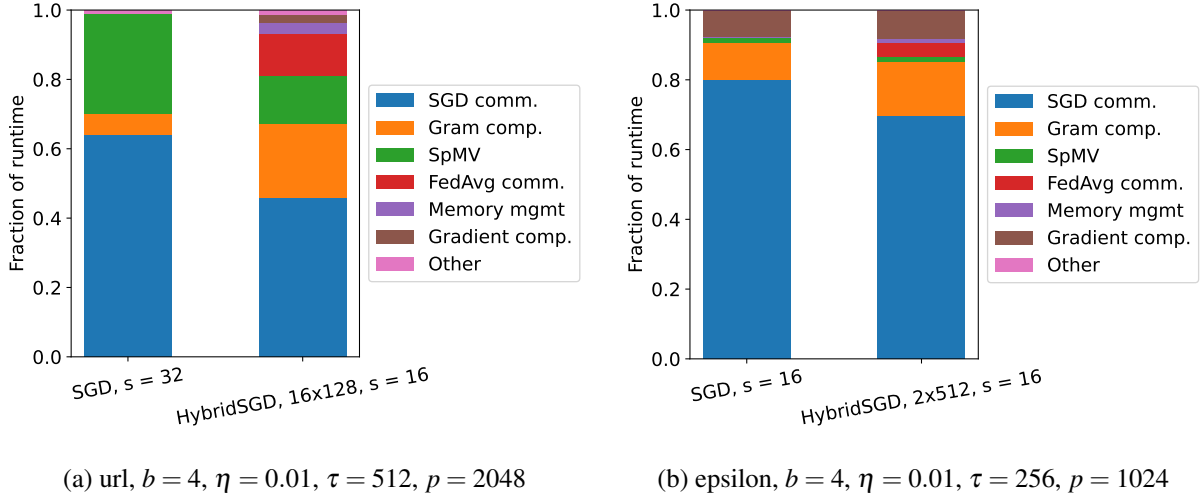


Figure 8: Runtime breakdown of s -step SGD

on the values of s and τ . We report results with settings that achieved the best running times for SGD and HybridSGD. The results from the s -step SGD experiments illustrate that at $p = 2048$, a large fraction of runtime is spent in communication (64.2%), while computation accounts for a smaller fraction (35.8%). Note that the Gram matrix computation time accounts for 6.1% of the runtime. In comparison, HybridSGD spent 57.9% of the runtime performing communication and 42.1% performing computation (and overhead). In Figure 8a, a 2D processor grid with dimensions $p_r = 16$ and $p_c = 128$ was optimal, where 16 row teams performed FedAvg with a communication delay of $\tau = 512$ iterations. Given this large value of τ , FedAvg communication accounts for only a small fraction of communication (12% vs. 45.9% for s -step SGD communication). HybridSGD also alleviates load imbalance in the SpMV computation due to the addition of row partitioning, which reduced the fraction of time spent performing SpMVs to 13.9% of total runtime. This decrease in SpMV runtime, however, is offset by the Gram matrix computation, which accounts for 21.3% of total runtime. This is an increase of $3.5\times$ over the Gram computation fraction from s -step SGD. Note, however, that this increase in time spent on Gram computation is expected since HybridSGD performs $p_r = 16$ simultaneous s -step SGD calls that are parallelized over $p_c = 128$ processors instead of parallelizing over $p = 2048$ processors for s -step SGD (a $16\times$ decrease in parallelism during Gram computation). The remaining fraction of runtime (6.9%) is spent on memory management (e.g. zeroing buffers and creating/destroying MKL sparse matrix handles), gradient computation (e.g. s -step gradient corrections and other vector operations), and other computation (e.g. overhead). Memory management, gradient computation, and other computation account for 3.3%, 2.2%, and 1.4% of the total runtime, respectively.

In Figure 8b, we show the runtime breakdown of s -step SGD ($s = 16$) and HybridSGD ($s = 16$) for the dense, epsilon dataset with $p = 1024$. Due to the dense input, SpMV computations are load-balanced for both algorithms, therefore, communication accounts for a larger fraction of runtime for s -step SGD and HybridSGD (80.1% and 73.7%, respectively). The remaining 19.9% of runtime for s -step SGD is spent on computation which is composed of Gram computation (10.4%), SpMV (1.8%), and gradient computation (7.7%). Note that the gradient computation involves dense matrix-vector products and additional vector operations in order to perform s -step corrections. In contrast, HybridSGD spent 26.3% of runtime on computation which is divided into Gram computation (15.5%), SpMV (1.6%), memory management (1.1%), and gradient computation (8.1%). Since HybridSGD performs $p_r = 2$ simultaneous s -step SGD calls which are parallelized across $p_c = 512$ processors, we expect the Gram matrix computation to represent a factor of $2\times$ larger fraction of runtime than for s -step SGD with $p = 1024$. For HybridSGD on the epsilon dataset,

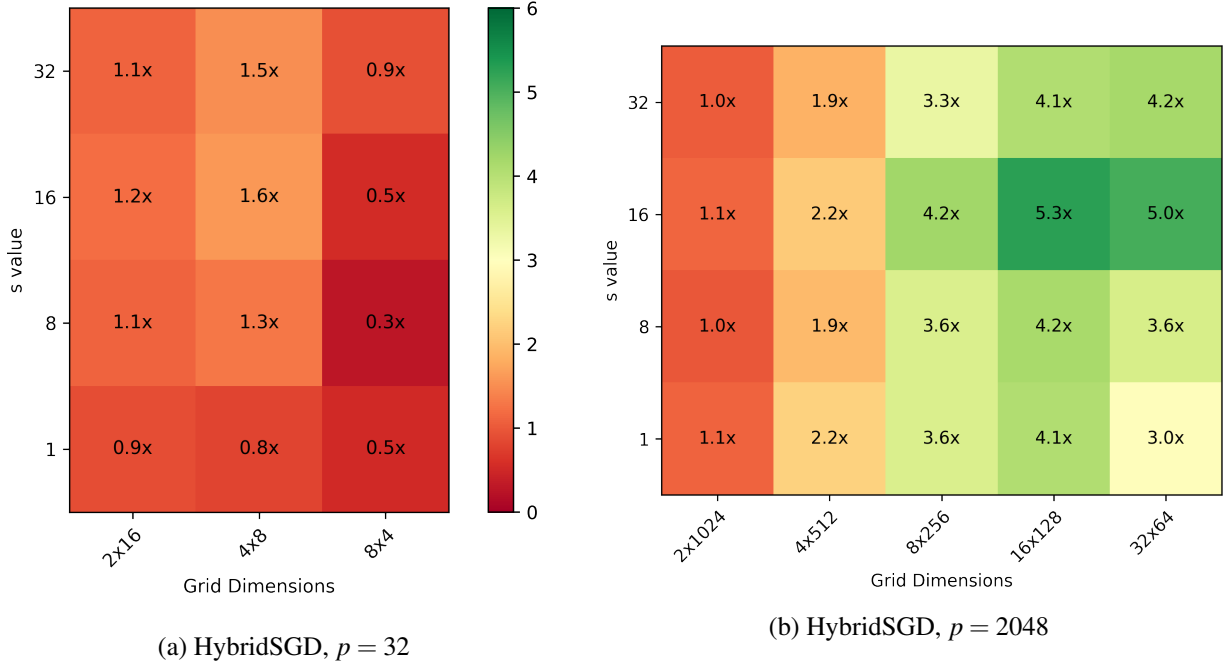


Figure 9: Speedup heatmaps of HybridSGD at $p = 32$ (Figure 9a) and at $p = 2048$ (Figure 9b) for different values of $s \in \{1, 8, 16, 32\}$ and different grid dimensions. Speedups are calculated relative to the fastest runtime achieved by s -step SGD during the small batch size strong scaling study (see Figure 7a). We use the following hyperparameter settings: $b = 4$, $\eta = 0.01$, and $\tau = 512$.

Gram computation represents a factor of $1.5\times$ larger fraction of runtime than for s -step SGD.

6.4 Processor Grid Tuning

Figure 9 shows a comparison of the speedups attained by HybridSGD for various settings of s and grid dimensions on the url dataset at two different scales: at $p = 32$ (Figure 9a) and $p = 2048$ (Figure 9b). The experiments were conducted using the hyperparameter settings described in the small batch size ($b = 4$) setting for the url dataset (see Figure 7a). The speedups are relative to the fastest running time achieved by s -step SGD from Figure 7a, which corresponds to a runtime of 8.3895 seconds at $p = 32$ and $s = 16$. Speedups along the y -axis are achieved by avoiding communication through the use of s -step SGD with increasing values of s (note that $s = 1$ corresponds to 1D-column partitioned parallel SGD in Tables 1 and 2). Speedups along the x -axis are achieved by increasing the number of processor row teams (p_r) which perform FedAvg with $\tau = 512$. At small scale, in Figure 9a, we observe that HybridSGD attains a maximum speedup of $1.6\times$ with the settings $s = 16$ and grid dimension ($p_r = 4, p_c = 8$). The benefit of increasing s is limited at $p_r = 2$ due to load imbalance, so speedup (from $s = 8$ to $s = 16$) is limited to approximately a 10% improvement in runtime. However, once load imbalance is reduced at $p_r = 4$, we observe a speedup of $2\times$ when comparing $s = 16$ relative to $s = 1$. For the experiments with $p_r = 8$, we observed a significant ($5.9\times$) increase in time spent in communication corresponding to weight vector averaging in FedAvg than when compared to $p_r = 4$ and $s = 16$. A $2\times$ increase in p_r results in a proportional increase in computation, bandwidth, and latency (see Tables 1 and 2), along with the increased potential for convergence delay through increased use of FedAvg. At large scale, in Figure 9b, HybridSGD attains a maximum speedup of $5.3\times$ at $s = 16$ and $p_r = 16$. Note that in this setting, $p_r > 2$ achieves larger speedups at $s = 1$ than what we observed at small scale ($p = 32$). This indicates that load imbalance is the primary

barrier to achieving faster runtimes than communication cost at this scale. However, once load imbalance is alleviated (at $p_r = 16$), we observed a speedup of $1.23\times$ at $s = 16$ when compared to $s = 1, p_r = 16$. Note that lower speedups from s -step SGD speedups should be expected since p_c becomes smaller (where latency is not as dominant) which results in a proportional increase in computation as the local weight vector is of dimension n/p_c . In summary, we show in this experiment that HybridSGD allows a continuous tradeoff between s -step SGD (y-axis) and FedAvg (x-axis) and provides more opportunities to reduce running time than those enabled by s -step SGD or FedAvg alone.

7 Conclusion

This work designed, analyzed, and implemented a communication-efficient 2D parallel SGD method that generalizes existing 1D, communication-efficient SGD variants. We showed that our HybridSGD variant achieved speedups up to $5.3\times$ over the existing state-of-the-art and enables $2\times$ more scalability on a modern, Cray EX supercomputing cluster. Our design primarily focused on a convex, binary classification task, however, the approach applies to other convex loss functions where s -step methods apply (such as regularized least-squares, LASSO, SVM, and kernelized variants of SVM and least-squares methods). One of the primary areas of future work is to develop a PyTorch-based, GPU-accelerated variant of HybridSGD with the aim of reducing communication during distributed-memory training of deep neural networks using SGD-based optimizers.

Acknowledgements

Thanks to Grey Ballard for numerous, helpful discussions on this work. This work was supported by the U.S. Department of Energy, Office of Science, Advanced Scientific Computing Research (ASCR) program under Award Number DE-SC-0023296. This research used resources of the National Energy Research Scientific Computing Center (NERSC), a Department of Energy Office of Science User Facility using NERSC award ASCR-ERCAP0026261 and ASCR-ERCAP0028617.

References

- [1] E. Carson. *Communication-avoiding Krylov subspace methods in theory and practice*. PhD thesis, EECS Department, University of California, Berkeley, Aug. 2015.
- [2] E. Carson and J. Demmel. A residual replacement strategy for improving the maximum attainable accuracy of s-Step Krylov subspace methods. *SIAM Journal on Matrix Analysis and Applications*, 35(1):22–43, 2014.
- [3] E. Carson and J. Demmel. Accuracy of the s-Step Lanczos method for the symmetric eigenproblem in finite precision. *SIAM Journal on Matrix Analysis and Applications*, 36(2):793–819, 2015.
- [4] E. Carson, N. Knight, and J. Demmel. An efficient deflation technique for the communication-avoiding conjugate gradient method. *Electron. Trans. Numer. Anal.*, 43:125–141, 2014-2015.
- [5] C.-C. Chang and C.-J. Lin. Libsvm: A library for support vector machines. *ACM transactions on intelligent systems and technology (TIST)*, 2(3):27, 2011.
- [6] A. Chronopoulos. *A Class of Parallel Iterative Methods Implemented on Multiprocessors*. Ph.D., University of Illinois at Urbana-Champaign, United States – Illinois, 1987.

- [7] A. T. Chronopoulos. s-Step Iterative Methods for (Non)Symmetric (In)Definite Linear Systems. *SIAM Journal on Numerical Analysis*, 28(6):1776–1789, Dec. 1991.
- [8] A. T. Chronopoulos and C. W. Gear. On the efficient implementation of preconditioned s-step conjugate gradient methods on multiprocessors with memory hierarchy. *Parallel computing*, 11(1):37–53, 1989.
- [9] A. T. Chronopoulos and C. D. Swanson. Parallel iterative S-step methods for unsymmetric linear systems. *Parallel Computing*, 22(5):623–641, Aug. 1996.
- [10] G. Chávez, Y. Liu, P. Ghysels, X. S. Li, and E. Rebrova. Scalable and Memory-Efficient Kernel Ridge Regression. In *2020 IEEE International Parallel and Distributed Processing Symposium (IPDPS)*, pages 956–965, May 2020.
- [11] A. Devarakonda. *Avoiding Communication in First Order Methods for Optimization*. PhD thesis, EECS Department, University of California, Berkeley, Jul 2018.
- [12] A. Devarakonda and J. Demmel. Avoiding Communication in Logistic Regression. In *2020 IEEE 27th International Conference on High Performance Computing, Data, and Analytics (HiPC)*, pages 91–100, Dec. 2020.
- [13] A. Devarakonda, K. Fountoulakis, J. Demmel, and M. W. Mahoney. Avoiding Synchronization in First-Order Methods for Sparse Convex Optimization. In *2018 IEEE International Parallel and Distributed Processing Symposium (IPDPS)*, pages 409–418. IEEE, 2018.
- [14] A. Devarakonda, K. Fountoulakis, J. Demmel, and M. W. Mahoney. Avoiding Communication in Primal and Dual Block Coordinate Descent Methods. *SIAM Journal on Scientific Computing*, 41(1):C1–C27, Jan. 2019.
- [15] W. Gropp, E. Lusk, and A. Skjellum. *Using MPI: Portable Parallel Programming with the Message-Passing Interface*. The MIT Press, 2014.
- [16] M. F. Hoemmen. *Communication-avoiding Krylov subspace methods*. PhD thesis, EECS Department, University of California, Berkeley, Apr. 2010.
- [17] Intel. Intel® oneAPI Programming Guide. <https://www.intel.com/content/www/us/en/docs/oneapi/programming-guide/2025-0/overview.html>. Accessed: 2024-12-02.
- [18] S. Kim and A. Chronopoulos. An efficient nonsymmetric Lanczos method on parallel vector computers. *Journal of Computational and Applied Mathematics*, 42(3):357–374, 1992.
- [19] C. Ma, J. Konečný, M. Jaggi, V. Smith, M. I. Jordan, P. Richtárik, and M. Takáč. Distributed optimization with arbitrary local solvers. *Optimization Methods and Software*, 32(4):813–848, 2017.
- [20] NERSC. Architecture - NERSC Documentation. <https://docs.nersc.gov/systems/perlmutter/architecture/>. Accessed: 2024-12-02.
- [21] F. Niu, B. Recht, C. Re, and S. J. Wright. HOGWILD! a lock-free approach to parallelizing stochastic gradient descent. In *Proceedings of the 24th International Conference on Neural Information Processing Systems, NIPS’11*, pages 693–701, Red Hook, NY, USA, Dec. 2011. Curran Associates Inc.
- [22] R. Rabenseifner. Optimization of Collective Reduction Operations. In M. Bubak, G. D. van Albada, P. M. A. Sloot, and J. Dongarra, editors, *Computational Science - ICCS 2004*, pages 1–9, Berlin, Heidelberg, 2004. Springer.

- [23] S. Sallinen, N. Satish, M. Smelyanskiy, S. S. Sury, and C. Ré. High Performance Parallel Stochastic Gradient Descent in Shared Memory. In *2016 IEEE International Parallel and Distributed Processing Symposium (IPDPS)*, pages 873–882, May 2016.
- [24] Z. Shao and A. Devarakonda. Scalable Dual Coordinate Descent for Kernel Methods, June 2024. arXiv:2406.18001 [cs, stat].
- [25] V. Smith, S. Forte, C. Ma, M. Takáč, M. I. Jordan, and M. Jaggi. CoCoA: A general framework for communication-efficient distributed optimization. *Journal of Machine Learning Research*, 18(230):1–49, 2018.
- [26] S. Soori, A. Devarakonda, Z. Blanco, J. Demmel, M. Gurbuzbalaban, and M. M. Dehnavi. Reducing communication in proximal Newton methods for sparse least squares problems. In *Proceedings of the 47th International Conference on Parallel Processing*, pages 1–10, 2018.
- [27] S. U. Stich. Local SGD converges fast and communicates little. In *International Conference on Learning Representations*, 2019.
- [28] R. Thakur, R. Rabenseifner, and W. Gropp. Optimization of collective communication operations in MPICH. *International Journal of High Performance Computing Applications*, 19(1):49–66, Feb. 2005.
- [29] S. Williams, M. Lijewski, A. Almgren, B. V. Straalen, E. Carson, N. Knight, and J. Demmel. s-Step Krylov subspace methods as bottom solvers for geometric multigrid. In *IEEE international parallel and distributed processing symposium*, pages 1149–1158, May 2014.
- [30] Y. You, J. Demmel, K. Czechowski, L. Song, and R. Vuduc. CA-SVM: Communication-Avoiding Support Vector Machines on Distributed Systems. In *2015 IEEE International Parallel and Distributed Processing Symposium*, pages 847–859, May 2015.
- [31] Y. You, X. Lian, J. Liu, H.-F. Yu, I. S. Dhillon, J. Demmel, and C.-J. Hsieh. Asynchronous Parallel Greedy Coordinate Descent. In *Advances in Neural Information Processing Systems*, volume 29. Curran Associates, Inc., 2016.
- [32] Z. A. Zhu, W. Chen, G. Wang, C. Zhu, and Z. Chen. P-packSVM: Parallel primal grAdient desCent kernel SVM. In *Proceedings of the 9th IEEE international conference on data mining*, pages 677–686, 2009.